

## Direct Visualization of Polypeptide Shell of Ferritin Molecule by Atomic Force Microscopy

Satomi Ohnishi,\* Masa-hiko Hara,<sup>‡</sup> Taiji Furuno,<sup>‡</sup> Takao Okada,<sup>§</sup> and Hiroyuki Sasabe\*<sup>‡</sup>

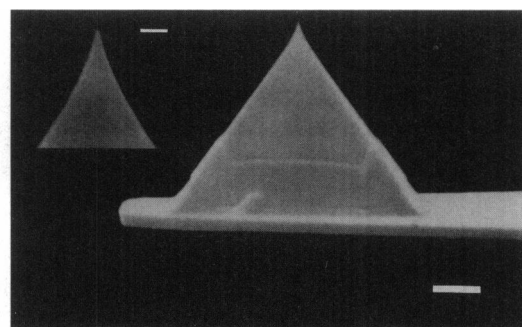
<sup>‡</sup>Frontier Research Program, The Institute of Physical and Chemical Research (RIKEN), Wako, Saitama 351-01, Japan; \*Department of Biological and Environmental Sciences, Saitama University, Urawa, Saitama 338, Japan; and <sup>§</sup>Olympus Optical Co., Ltd., Kuboyama-cho, Hachioji, Tokyo 192, Japan

**ABSTRACT** The polypeptide shell of the ferritin molecule has been imaged in water by atomic force microscopy (AFM). The central dip and the quaternary structure could be observed on the surface of the ferritin molecule anchored inhomogeneously in two dimensions. These structures observed in the AFM images are quite similar to the electron density map near the top of the apoferritin viewed down from a 4-fold axis structure reported previously (S. H. Banyard, D. K. Stammers, and P. M. Harrison. 1978. *Nature (Lond.)*. 271:282-284). It has been achieved by introducing a "self-screening effect" of the surface charges of the AFM sample (S. Ohnishi, M. Hara, T. Furuno, and H. Sasabe. 1992. *Biophys. J.* 63:1425-1431) and the specially sharpened stylus of AFM cantilever.

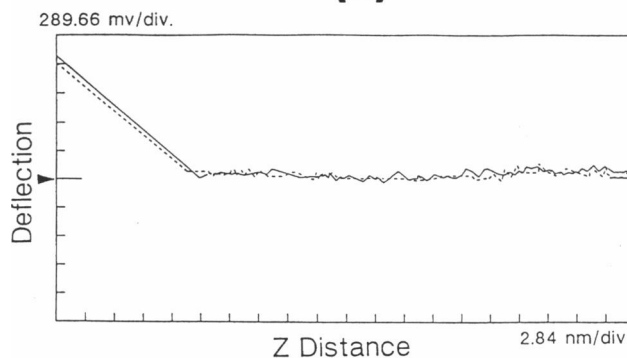
### INTRODUCTION

Since its conception (Binnig et al., 1986) atomic force microscopy (AFM) has been drawing increasing attention as a novel method that provides an outstanding capability for directly mapping the topological features of nonconductive biological specimens under physiological conditions. We now report the first use of the AFM to unambiguously image the surface structure of protein molecules by introducing the "self-screening effect" of the surface charges and the specially sharpened stylus. We have imaged individual protein ferritin molecules by the AFM in pure water, which was electrostatically deposited in a predesigned manner on a silicon surface, with clear discrimination against artifacts. Here we identify the presence of channels passing through the polypeptide shell which provide access routes for iron atoms forming an iron oxide core (Banyard et al., 1978). Our results highlight the remarkable potential of the AFM to visualize specific sites of soft biological macromolecules under newly developed nondestructive imaging conditions.

Currently, serious problems have been encountered in trying to obtain unambiguous AFM images of biological macromolecules in general, such as reliable immobilization methods for those molecules on atomically flat substrates, controlling the force acting on the sample surface, and the identification of images against artifacts. The molecules must not be packed into dense aggregates, but should be distributed in a two-dimensional (2D) plane, while moderate anchoring is required during scanning. Even if the molecule is found to form an ideal monolayer in two dimensions, the surface of the soft biological specimen is easily deformed by the strong force applied between stylus and specimen, even in the order of  $10^{-9}$  N, making the production of high-quality images difficult (Weisenhorn et al., 1989). Actually, clear AFM images of protein molecules have so far been restricted



(a)



(b)

**FIGURE 1** (a) Electron micrograph of the specially sharpened pyramidal  $\text{Si}_3\text{N}_4$  stylus on the cantilever fabricated by microcasting method (Albrecht et al., 1990). The cantilever is now commercially available from Olympus Optical Co. Wide scale bar indicates  $1.2 \mu\text{m}$  and narrow bar in enlarged view of the top,  $200 \text{ nm}$ . The pyramidal shape is determined by the silicon (111) planes with  $4\text{-}\mu\text{m}$  base width, and the top is sharpened by the low-temperature thermal oxidation process (Akamine and Quate, 1992). The vertex angle of the sharpened area from the top  $0.5 \mu\text{m}$  down is less than  $45$  degrees, and the tip radius is less than  $20 \text{ nm}$ . The cantilever used in this study is V-shaped and  $200 \mu\text{m}$  long, with a spring constant of  $0.021 \text{ N/m}$ . (b) Typical force curve for AFM imaging of ferritin monolayers in pure water obtained by combination of the "self-screening effect" with the sharpened stylus. The two curves are for approach (dashed line) and for withdrawal (solid line) of the stylus from the sample. The arrowhead indicates the operation point, where the force acting on the stylus can be successfully reduced to about  $10^{-11} \text{ N}$ , as estimated from this curve.

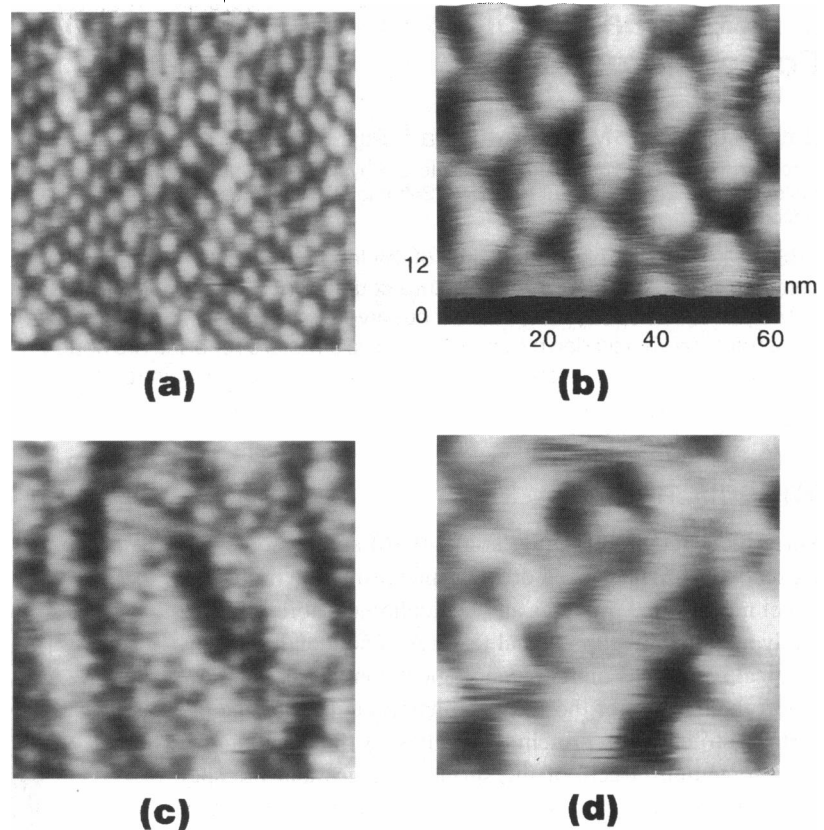
Received for publication 5 February 1993 and in final form 30 April 1993.

Address reprint requests to Satomi Ohnishi.

© 1993 by the Biophysical Society

0006-3495/93/08/573/05 \$2.00

**FIGURE 2** (a and b) AFM images of hexagonally close-packed ferritin molecules. (c and d) AFM images of inhomogeneous areas. Areas of images are  $210 \times 210$  nm (a and c) and  $63 \times 63$  nm (b and d). The AFM system used was a commercially available NanoScope II (Digital Instruments, Inc., Santa Barbara, CA). AFM images ( $400 \times 400$  pixels) were obtained using the "height mode," which kept the force constant at the operation point. Scanning drift was not reconstructed along the ordinate in a and b. In related AFM studies, we find no evidence of deformation of the packing structures or denaturation of ferritin molecules.



mainly to naturally formed 2D protein crystals, which are sufficiently stable (Butt et al., 1990; Hoh et al., 1991; Devaud et al., 1992).

In order to overcome such difficulties, we have demonstrated in a previous paper the first AFM imaging of artificially formed 2D arrays of water-soluble ferritin molecules bound to a charged polypeptide monolayer of poly-1-benzyl-L-histidine (PBLH) on a silicon surface (Ohnishi et al., 1992). The 2D arrays of proteins have been used for structural studies with clear discrimination against artifacts (Uzgiris and Kornberg, 1983). We discussed the AFM imaging from the viewpoint of controlling electrostatic force between stylus and sample surface and concluded that the cancellation of electrostatic charges at the interface of negatively charged ferritin and positively charged PBLH is one of the most effective factors in attaining low-force AFM imagings. By introducing such a "self-screening effect" of the surface charges of the AFM sample itself, the forces between stylus and protein monolayer could be kept sufficiently smaller than  $10^{-10}$  N, resulting in reproducible nondestructive imaging of the ordered array of ferritin molecules. In numerous such imagings, however, it has also been realized that image quality has still been affected by the shape of the stylus itself.

In addition to the "self-screening effect," here we have introduced the specially sharpened stylus to investigate more precise surface structures of ferritin.

## MATERIALS AND METHODS

Horse spleen ferritin (Sigma Chemical, St. Louis, MO) was dissolved in pure water and fractionated by ultracentrifugation several times at  $200,000 \times g$

for 40 min. The heavier fractions were diluted with a solution of sodium chloride (10 mM) to a final concentration of 100 mg/ml. The ferritin solution was diluted with phosphate buffer (5 mM, pH 5.3) and prepared to a concentration of  $30 \mu\text{g/ml}$ . The micro Langmuir trough ( $20 \text{ mm} \times 35 \text{ mm} \times 2 \text{ mm}$ ) was filled with the ferritin solution until the air-water interface had a slightly convex shape. PBLH (Sigma), with an average degree of polymerization of 100, was dissolved in chloroform containing dichloroacetic acid ( $0.68 \mu\text{l}$  to 1 mg of PBLH) to a concentration of  $0.54 \text{ mg/ml}$ . The desired amount ( $3 \mu\text{l}$ ) of PBLH was spread over the ferritin solution and allowed to incubate condensed ferritin monolayers at a ferritin-PBLH interface for 3 h at room temperature.

We used a silicon wafer (n-type, (100)) as the substrate. Before the film transfer, the silicon wafers were irradiated with UV light from a low-pressure mercury lamp to obtain hydrophilic surfaces, placed in a glass desiccator filled with hexamethyldisilazane vapor, and then heated to  $60^\circ\text{C}$  for 1 h to bind hexamethyldisilazanes covalently to the surface, forming the alkylated hydrophobic surface. The interfacial film (hetero-bilayer of ferritin-PBLH) on the trough was transferred onto such an alkylated silicon wafer by a horizontal transfer method. The ferritin-PBLH film transferred on a silicon wafer was rinsed with pure water. The film was imaged using a fluid cell in pure water.

The AFM system used in this study was a commercially available NanoScope II (Digital Instruments, Inc., Santa Barbara, CA). AFM images ( $400 \times 400$  pixels) were obtained using "height mode," which kept the force constant. Typical AFM parameters were as follows: integral gain = 3; proportional gain = 5; two-dimensional gain = 0.3; scan rate = 8.68–19.6 Hz; scan width = 10–700 nm. In order to obtain the best images, the applied force was minimized and stabilized by adjusting the height of cantilever (set point voltage) during the sample surface scan.

## RESULTS AND DISCUSSION

Horse spleen ferritin has an isoelectric point of about 4.5 and is negatively charged in a solution of pH 5 or above (Artbuthnott and Beely, 1975). The imidazole ring of PBLH, on

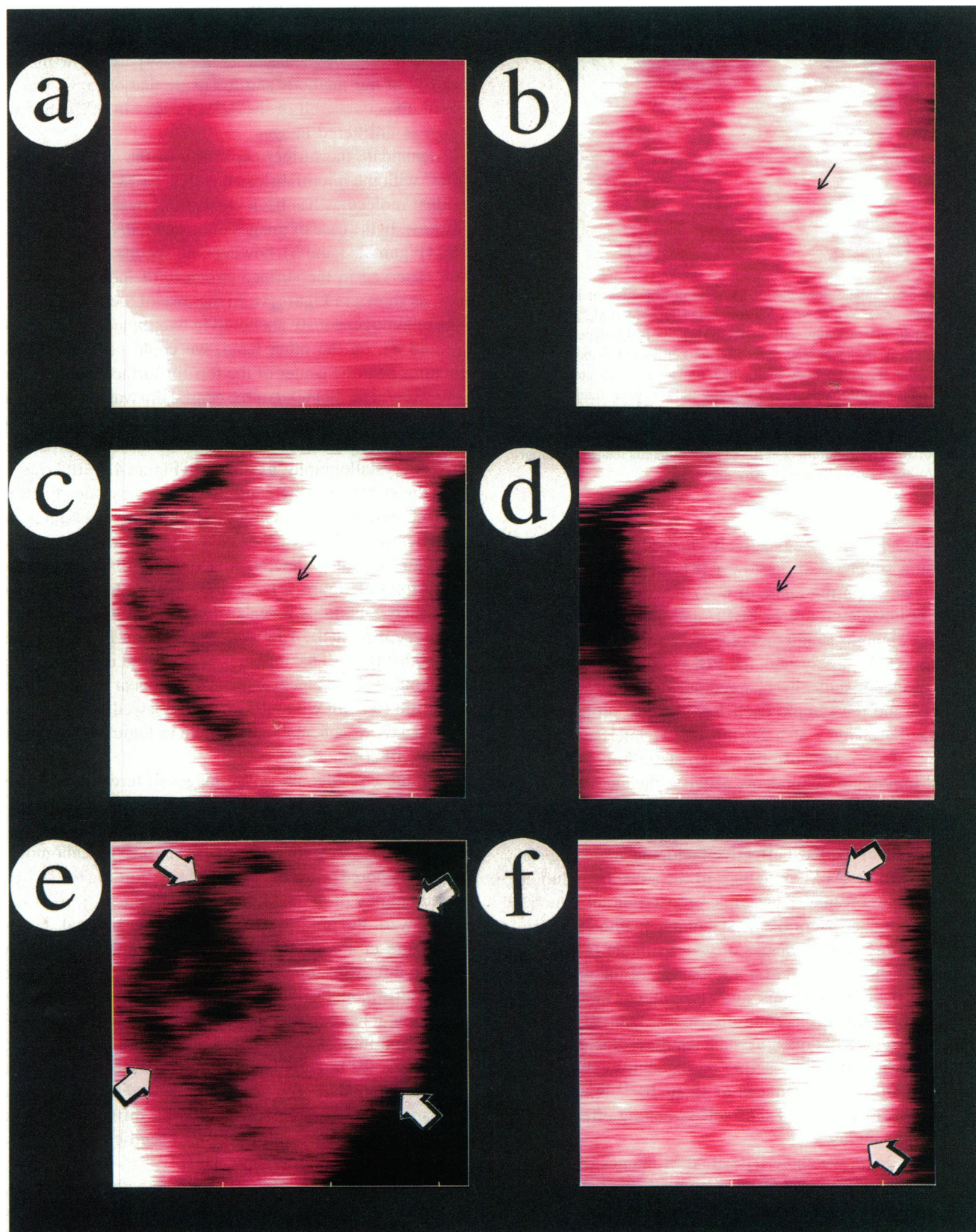


FIGURE 3 (a) AFM image of one ferritin molecule in hexagonally packed 2D arrays. No specific features have been observed. (b–f) AFM images of one ferritin molecule inhomogeneously anchored in two dimensions. These images of the ferritin molecule have a 12-nm diameter, while areas of images (a–e) are around  $15 \times 15$  nm. Zooming in to a smaller scan size (less than  $12 \times 12$  nm) was carried out in f. Diplike structure (arrows in b–d) and fourfold symmetry could be identified in inhomogeneously distributed ferritin, although flattening of the molecules might be taken into account.

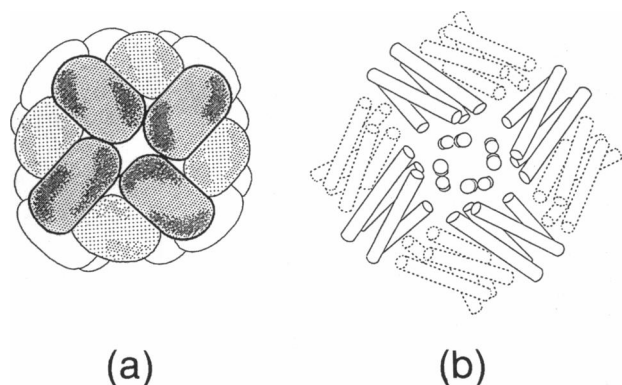


FIGURE 4 Schematic drawings of the subunit arrangement in an apoferritin molecule viewed down a fourfold axis (Banyard et al., 1978). (a) Complete molecular structure with a spherical shell of 24 polypeptide subunits. Centers of the quaternary structure are considered to be channels passing through the polypeptide shell which provide access routes for iron atoms forming an iron oxide core. Currently there is great interest in the structure and function of the outer shell itself, since the new application of ferritin has been reported as a reaction cavity for the preparation of inorganic nanometer particles (Meldrum et al., 1991). (b) Subunits related by a fourfold axis following the electron density map.

the other hand, should be positively charged, when PBLH is spread on a subphase at the lower pH than the pKa of the histidyl residue (in the range of 6–7). Therefore, positively charged imidazole groups of PBLH and negatively charged ferritin are thought to interact electrostatically in the range of pH 4.5–6.5. In this system, the PBLH film plays a crucial role as an electrostatically charged substrate to fix ferritin molecules, and the sample itself has intrinsic properties of canceling the charges at a ferritin-PBLH interface (“self-screening effect”). Because the electrostatic force is one of the most important components between the cantilever and the sample surface and is strongly affected by the surface charges, a screening of the surface charges should be considered as one of the most effective factors in achieving stabilized low-force AFM imagings in an aqueous solution. From this point of view, the sample preparation introducing “self-screening” is one of the most suitable methods for producing low-force AFM images of water-soluble proteins.

Figure 1a shows an electron micrograph of the microfabricated cantilever used in this study (Olympus Optical Co.), where the tip radius size is controlled to less than 20 nm. The typical force curve obtained by such cantilevers is shown in Figure 1b, where the force acting on the stylus can be successfully stabilized and reduced to about  $10^{-11}$  N, which is attained by combination of the “self-screening effect” with the sharpened stylus.

In Figure 2a–d, we show typical AFM images of ferritin molecules bound to a PBLH layer on a silicon surface obtained by the microfabricated stylus. Individually distinguishable spherical patterns are observed in different scanning areas. In numerous observations of the samples prepared under the suitable “self-screening effect” condition ( $\sim$ pH 5.3) (Ohnishi et al., 1992), large hexagonal 2D crystal domains of ferritin molecules could be imaged clearly (Fig-

ure 2, a and b), while some inhomogeneous areas were observed (Figure 2, c and d). Both distributions have also been confirmed in the same manner by high-resolution scanning electron microscopy (Furuno et al., 1989). To show the superiority of our methods and to ensure that our raw data be judged objectively, all of the AFM images in this paper are shown as unfiltered images.

To elucidate the further capability of the “self-screening effect” with the microfabricated stylus, AFM imaging of individual molecules has been carried out over a small scanning area. In the case of images of hexagonally packed molecules (Figure 2, a and b), however, no specific features have been observed in the surface structure of individual molecules, as shown in Figure 3a. In the case of the ferritin molecules inhomogeneously anchored in two dimensions (Figure 2, c and d), on the other hand, we could observe diplike structures near the center of the ferritin surface, as shown in Figure 3b–f. The diameter of the central dip was always about 1 nm. This result suggests the existence of channels, the size of which is in good agreement with the structure predicted by x-ray crystallography, as shown in Figure 4. Furthermore, under the stable imaging condition created by adjusting the feedback height of the cantilever to minimize the imaging drift after several scans, the quaternary structure could be identified, time after time, as four rods approximately 4 nm long (arrows in Figure 3e). Zooming in to a smaller scan size under such conditions reveals somewhat more details over the polypeptide shell of ferritin, as shown in Figure 3f. It is evident that the surface topography observed in the image is quite similar to the electron density map near the top of the apoferritin (ferritin without iron core) viewed from above a fourfold axis, as schematically shown in Figure 4b (reported by Banyard et al., 1978).

From these results, the AFM images of ferritin molecules can be clearly divided into two categories: no specific features on hexagonally packed molecules (Figure 3a) and diplike structures with four symmetrical rods on inhomogeneously anchored ones (Figure 3, b–f). According to electron crystallography of the 2D ferritin crystal, the projection image showed threefold symmetry in a hexagonal lattice (Yoshimura et al., 1990). In the case of inhomogeneously distributed ferritins, on the other hand, it has been expected that the ferritin molecules are bound in a fourfold symmetry. In addition, it has been suggested that contacts between subunits around fourfold axes are relatively tenuous, compared with those at the threefold axes (Banyard et al., 1978). Since the adjacent subunits contact tightly around threefold axes, it is natural that each subunit would be difficult to image separately by AFM, resulting in no specific features in a hexagonally packed arrangement.

Therefore, we propose here, following those structural analyses with different symmetry, that the diplike structure observed in inhomogeneously anchored molecules is not an artifact caused by scanning but a channel for iron atoms at the fourfold axis on the polypeptide shell surface. The different symmetry axis orientation of the ferritin core has been also observed by scanning tunneling microscopy (Yang et al.,

1992). We believe that our results demonstrate the remarkable possibility that the AFM can be used to visualize specific sites of soft biological macromolecules, which would be attained by combination of the "self-screening effect" of the surface charges with the newly designed stylus. Application of such nondestructive AFM imaging to other protein molecules is now in progress, and an extensive discussion will be reported elsewhere.

## REFERENCES

- Akamine, S., and C. F. Quate. 1992. Low temperature thermal oxidation sharpening of microcast tips. *J. Vac. Sci. Technol. B*. 10:2307–2310.
- Albrecht, T. R., S. Akamine, T. E. Carver, and C. F. Quate. 1990. Microfabrication of cantilever styli for the atomic force microscope. *J. Vac. Sci. Technol. A*. 8:3386–3396.
- Arbuthnott, J. P., and J. A. Beely. 1975. *Isoelectric Focusing*. Butterworths, London. 125 pp.
- Banyard, S. H., D. K. Stammers, and P. M. Harrison. 1978. Electron density map of apoferritin at 2.8-Å resolution. *Nature (Lond.)*. 271:282–284.
- Binnig, G., C. F. Quate, and C. Gerber. 1986. Atomic force microscope. *Phys. Rev. Lett.* 56:930–933.
- Butt, H.-J., K. H. Downing, and P. K. Hansma. 1990. Imaging the membrane protein bacteriorhodopsin with the atomic force microscope. *Biophys. J.* 58:1473–1480.
- Devaud, G., P. S. Furciniti, J. C. Fleming, M. K. Lyon, and K. Douglas. 1992. Direct observation of defect structure in protein crystals by atomic force and transmission electron microscopy. *Biophys. J.* 63:630–638.
- Furuno, T., H. Sasabe, and K. Ulmer. 1989. Binding of ferritin molecules to a charged polypeptide layer of poly-1-benzyl-L-histidine. *Thin Solid Films*. 180:23–30.
- Hoh, J. H., R. Lal, S. A. John, J.-P. Revel, and M. F. Arnsdorf. 1991. Atomic force microscopy and dissection of gap junction. *Science (Washington DC)*. 253:1405–1408.
- Meldrum, F. C., V. J. Wade, D. L. Nimmo, B. R. Heywood, and S. Mann. 1991. Synthesis of inorganic nanophase materials in supramolecular protein cages. *Nature (Lond.)*. 349:684–687.
- Ohnishi, S., M. Hara, T. Furuno, and H. Sasabe. 1992. Imaging the ordered arrays of water-soluble protein ferritin with the atomic force microscope. *Biophys. J.* 63:1425–1431.
- Uzgiris, E. E., and R. D. Kornberg. 1983. Two-dimensional crystallization technique for imaging macromolecules, with application to antigen-antibody-complement complexes. *Nature (Lond.)*. 301:125–129.
- Weisenhorn, A. L., P. K. Hansma, T. R. Albrecht, and C. F. Quate. 1989. Forces in atomic force microscopy in air and water. *Appl. Phys. Lett.* 54:2651–2653.
- Yang, J., K. Takeyasu, A. P. Somlyo, and Z. Shao. 1992. Scanning tunneling microscopy of an ionic crystal: ferritin core. *Ultramicroscopy*. 45:199–203.
- Yoshimura, H., M. Matsumoto, S. Endo, and K. Nagayama. 1990. Two-dimensional crystallization of proteins on mercury. *Ultramicroscopy*. 32:265–274.